Reconstruction of Building Models from Maps and Laser Altimeter Data

U. Stilla, K. Jurkiewicz

Research Institute of Optronics and Pattern Recognition (FGAN-FOM)
Eisenstockstr. 12, D-76275 Ettlingen, Germany
usti@fom.fgan.de

Abstract. In this paper we describe a procedure for generating building models from large scale vector maps and laser altimeter data. First the vector map is analyzed to group the outlines of buildings and to obtain a hierarchical description of buildings or building complexes. The base area is used to mask the elevation data of single buildings and to derive a coarse 3D-description by prismatic models. Afterwards, details of the roof are analyzed. Based on the histogram of heights, flat roofs and sloped roofs are discriminated. For reconstructing flat roofs with superstructures, peaks are searched in the histogram and used to segment the height data. Compact segments are examined for a regular shape and approximated by additional prismatic objects. For reconstructing sloped roofs, the gradient field of the elevation data is calculated and a histogram of orientations is determined. Major orientations in the histogram are detected and used to segment the elevation image. For each segment containing homogeneous orientations and slopes, a spatial plane is fitted and a 3D-contour is constructed. In order to obtain a polygonal description, adjacent planes are intersected and common vertices are calculated.

1 Motivation

Three-dimensional city models find more and more interest in city and regional planning (Danahy, 1997). They are used for visualization (Gruen, 1998)(Gruber et al., 1997), e.g. to demonstrate the influence of a planned building to the surrounding townscape. Furthermore there is a great demand for such models in civil and military mission planning, disaster management (Kakumoto et al., 1997) and as basis for simulation e.g. in the fields of environmental engineering for microclimate investigations (Adrian & Fiedler, 1991) or telecommunications for transmitter placement (Kürner et al., 1993).

In industrial countries during the last years many maps have been stored digitally and additionally are available in vector form. Large scale topographical maps or cadastral maps show ground plans with no information on the height of buildings or shape of the roof. So far, information on height was derived from manual surveys or from stereo pairs of aerial images.

P.Agouris and A. Stefanidis (Eds.): ISD'99, LNCS1737, pp. 34-46, 1999

1.1 Laser Altimeter Data

Nowadays elevation data are commercially available from airborne laser scanners. Knowing the precise position and orientation of the airborne platform from differential Ground Positioning System (dGPS) and Inertial Navigation System (INS) measurements, the geographic position of the surface points in three spatial dimensions can be calculated to decimeter accuracy (Huising & Pereira, 1998). With current systems, points can be measured at approximately one point each 0.5 x 0.5 m^2 (Lohr, 1998). The sampled surface points distributed over a strip of 250-500m width allows the generation of a geocoded 2D array with elevation data in each cell (elevation image)(Fig. 1). Single flight strips are merged to a consistent digital surface model (DSM) of the whole survey area.

The run-time of a laser pulse reflected at the ground is used to calculate the distance between the sensor and a surface of the scene. If the laser beam illuminates a tree so multiple reflections at different ranges may occur. A certain percentage of the laser beam will be reflected by branches and leaves of the tree. Other parts will penetrate the foliage and will be finally reflected by the terrain surface. The reflected signal can be recorded and analyzed in *first pulse* or *last pulse* mode. While first pulse registration is the optimum choice when surveying the top of objects (e.g. canopy), last pulse registration should be chosen if the final elevation model should describe the ground surface. Fig. 1a shows a section of an image taken in first pulse mode in October. The foliage of the trees is visible. Fig. 1b was taken in last pulse mode in January. The branches and foliage are not visible and the building areas are smaller than in Fig 1a. In some areas no response could be received due to frost and ice. For the reconstruction of roofs we use the images of first pulse registration with a xy resolution of 1 m^2.

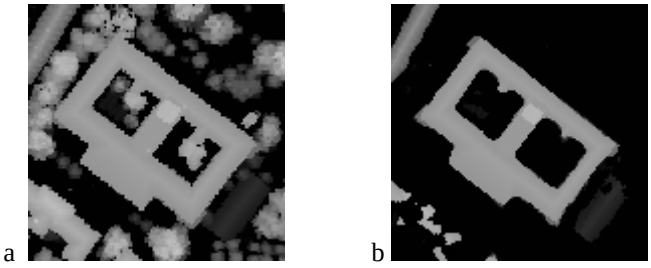

Fig. 1. . Elevation data taken in (a) first pulse mode and (b) last pulse mode.

1.2 Visualization

A simple way to visualize the elevation data is to assign a brightness value to the z-coordinate of each raster element. Combining this brightness with the z-coordinate in a 3D view leads to a plastic appearance of the raster data (Fig. 2). A more realistic appearance can be obtained by using an aerial image to texture the elevation data (Fig.

3). Nevertheless, the direct use of raster data has its limits for the purpose of a photorealistic animation or a geometric database of physical simulations or a query to an information system. First, the effort for storage and manipulation of data is high and second, an explicit description of the scene by objects, e.g. building models, is not available.

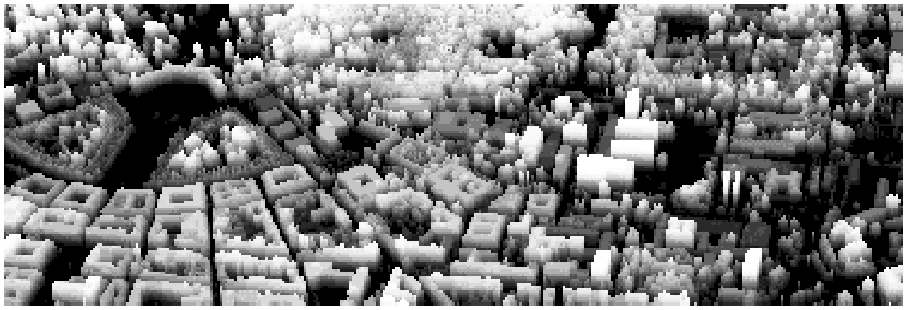

Fig. 2. 3D view of laser altimeter data (Karlsruhe, Germany).

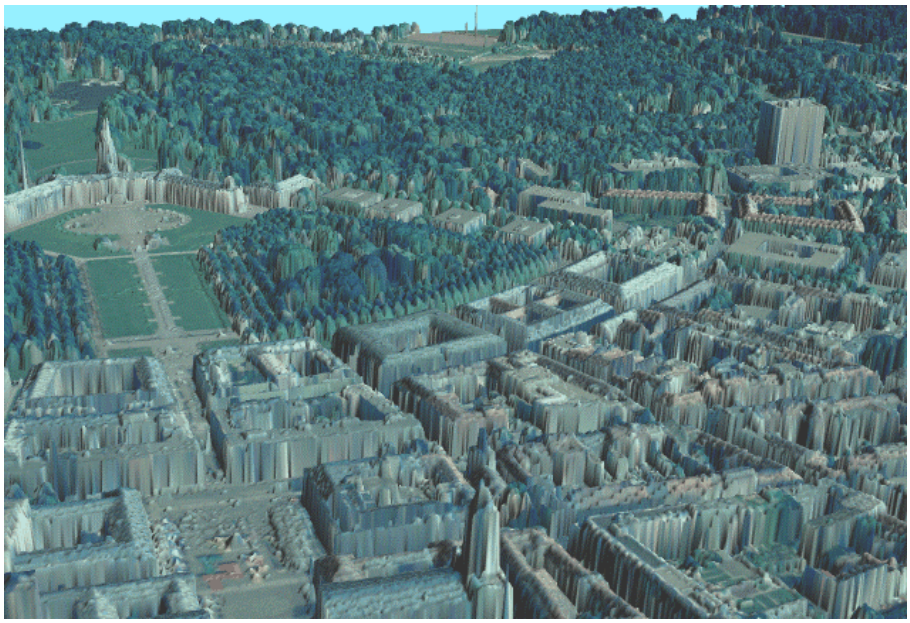

Fig. 3. 3D view of laser altimeter data textured by an aerial image.

1.3 Approaches for Automation

The manual construction and update of 3D building models is time consuming and expensive. That is why some authors propose approaches to automate the process of exploiting elevation data. In contrast to semi-automatic approaches (Gruen,

1998)(Guelch, 1997) we pursue approaches which allow a fully automatic reconstruction of buildings.

A detection of surface areas belonging to buildings is shown in Hug & Wehr (1997) by morphological filtering of laser images and examining local elevation histograms. The reflectivity obtained by processing the return signal energy is additionally used to separate segments of artificial objects from vegetation. Polygonal 3D-descriptions of buildings were not derived.

A polygonal description of a building is generated by the approach of Weidner & Förstner, (1995) using geometric constraints in form of parametric and prismatic models. The shape of buildings was limited to flat roofs or symmetric sloped gable roofs.

The reconstruction of more complex roof shapes can be found in (Haala and Brenner, 1997). A ground plan of a building is used to derive roof hypotheses. However, any roof construction based on this approach provides incorrect results if the roof structure inside the ground polygon does not follow the cues that can be obtained from the ground polygon (Haala and Brenner, 1997).

In our approach we also combine elevation data and map data to extract buildings - but the map data is not used to reconstruct the building roof.

2 Scene Analysis

The automatic generation of urban scene descriptions consists of a multistage process, using different information sources as maps, elevation data, aerial images. We describe structural relations of the object models by rules or so-called productions. The hierarchical organization of object concepts and productions can be depicted by a production net which - comparable to semantic networks - displays the part-of hierarchies of object concepts. Production nets are preferably implemented in a blackboard architecture in the environment system BPI (Blackboard-based Production System for Image Understanding, see Stilla, 1995).

In a first step we analyze the digital map by means of a production net in order to obtain a simple urban model consisting of prismatic objects.

3 Prismatic Objects

We use a large scale vector map which is organized in several layers, each of which contains a different class of objects (e.g. streets, buildings, etc.). Fig. 4a-c show a section of the scene, the large scale raster map (1:5000) and the layer *buildings* of the vector map. The topological properties connectivity, closedness, and containment of the non-ordered set of map-lines are tested by a production net of a generic model.

The aim of the analysis is to separate parts of buildings, to determine encapsulated areas and to group parts of buildings. The output of the analysis is a hierarchical description of the buildings or complexes of buildings (Stilla & Michaelsen, 1997).

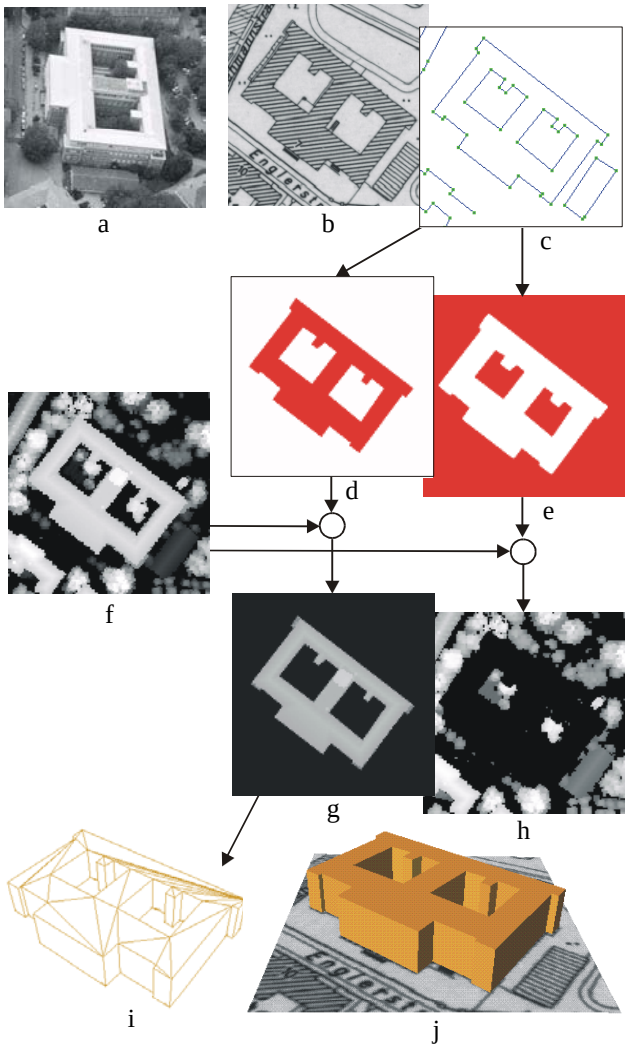

Fig. 4. Generation of prismatic objects from maps and elevation data

The result of the first step is used to mask the elevation data (Fig. 4f). In this way we obtain different elevation data for buildings (Fig. 4g) and non-buildings (surrounding)(Fig. 4h). Due to the fact that we use a buffer zone of some pixels (don't-care-area) along the polygon of the building contour, the negative building mask (Fig. 4e) is not the complement of the positive building mask (Fig. 4d).

For each building object of the map, a coarse 3D-description is constructed by a prismatic model. Depending on the task, the height of the covering plane can be calculated from the histogram using the (i) mean, (ii) median (for suppression of distortions), (iii) minimum (to get the height of the eaves) or (iv) maximum (to obtain the bounding box). This resulting wire-frame models is transformed into a surface model (Fig 4i,j) using an automatic triangulation.

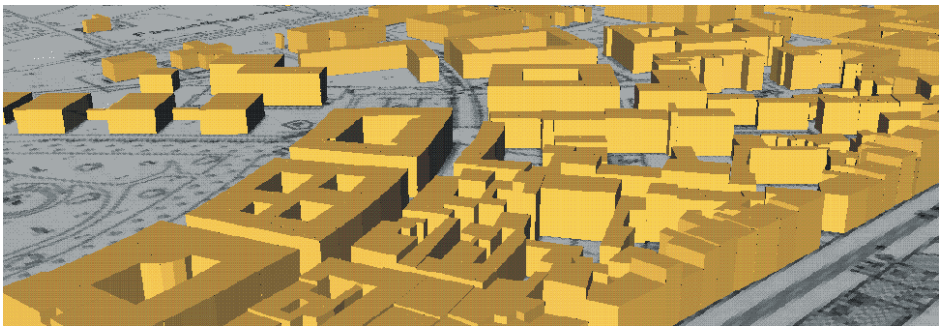

Fig. 5. City model of prismatic objects (buildings).

4 Roof Reconstruction

Depending on the task a more detailed description of the buildings as such models shown in Fig. 5 is required. The roof has to be reconstructed from elevation data. Simple roof structures show characteristic histograms (Fig. 6).

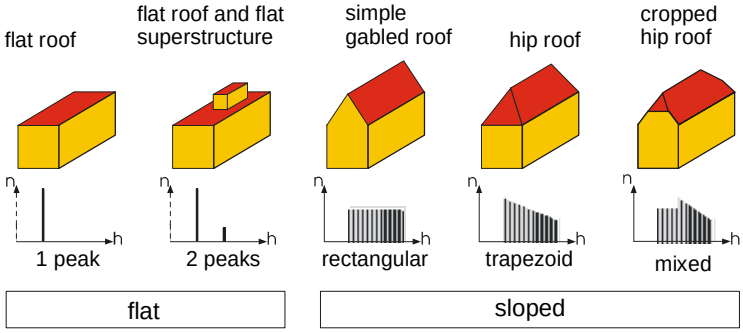

Fig. 6. Characteristic height histograms of simple roofs.

Flat roofed buildings show a significant peak in the histogram (Fig. 6a). The high of the peak (peak area) is given by the base area. If a flat roofed building has a flat superstructure (e.g. penthouse, air conditioning or elevator equipment) the histogram shows an additional peak above the main peak (Fig. 6b). Simple gabled roofs show a rectangular histogram (Fig. 6c). Assuming the same base area, the width of the rectangle depends on the slope of the roof. A hip roof shows a trapezoidal histogram

(Fig. 6d). The length of the ridge determines the height of the right side of the histogram. A cropped hip roof shows a mixture of a rectangle and a trapezoid form (Fig. 6e). Since the ideal histogram forms are not present in real data, the discrimination of different sloped roofs by their histograms will generally not be possible.

4.1 Roof Hypotheses

Based on the histogram of heights flat roofs and sloped roofs are discriminated. If the distance between minimum and maximum height is smaller than a threshold, a flat roof is hypothesized (i). If the distance is large enough, the distribution is examined by the entropy relative to the elevation range. If this value is low, a flat roof with a flat superstructure is hypothesized (ii), otherwise sloped roof parts are assumed (iii).

4.2 Flat Roofs

In the case of (i) the position of the peak's maximum is searched and is assigned as the height value to the prismatic object. In the case of (ii) the minor peaks with a certain gap to the main peak are looked for (Fig. 7c). Between the peaks a minimum is searched and a threshold value is calculated. These thresholds are used to segment the elevation data (Fig. 7d-f). The segments are labeled and examined for compactness (circumference/area). Segments, which are too small or not compact, are not taken into consideration for further analysis (Fig. 7e). A compact segment of a size greater than a minimum area confirms the hypothesis (Fig. 7f) and the contour is accepted (Fig. 7g).

In the following vectorization step of the contour chain we first try to fit the contour by a rectangle (Fig. 7h). If the assessment of the fit is lower than a given threshold the contour is rotated to a coordinate system parallel to the major orientation of the building. After projecting the contour points to the coordinate axes, peaks are searched in the histogram to describe the contour by a right-angled polygon (e.g. L-structure). If this approximation is insufficient as well, the contour is approximated by a dynamic split algorithm (Stilla et al., 1996).

4.3 Sloped Roofs

Some buildings show a mixture of sloped and flat parts of the roof (Fig. 8). Additionally, there may occur parts of a building e.g., garage, terrace, balcony, canopy of the front door, etc. They are not assigned to the main roof, because there height is much lower.

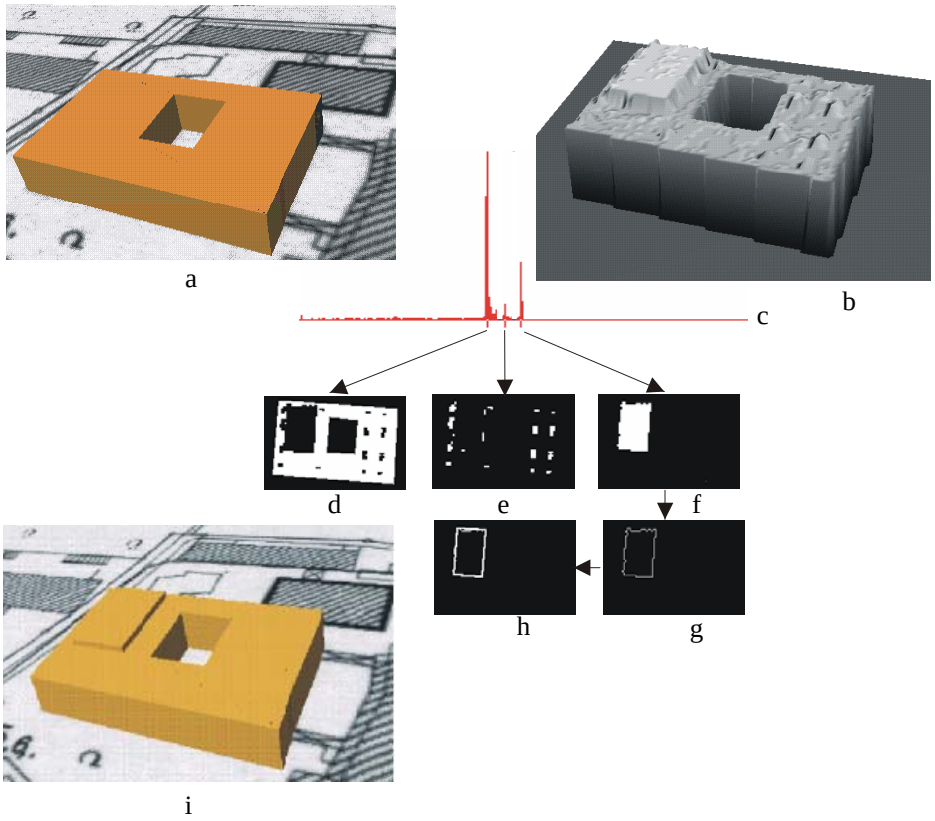

Fig. 7. Reconstruction of a flat superstructure.

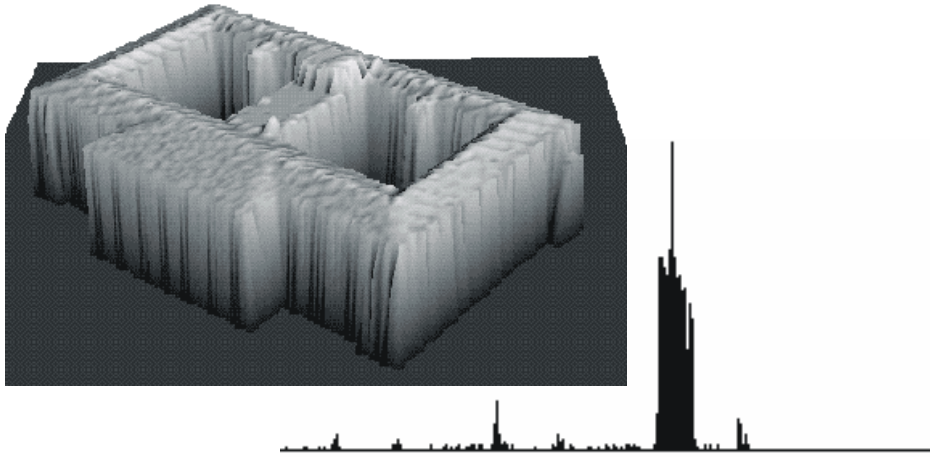

Fig. 8. 3D view of elevation data of a single building and the corresponding histogram.

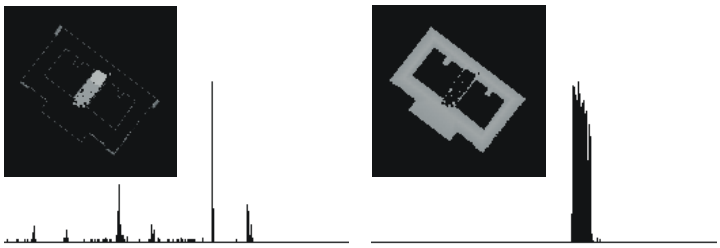

Fig. 9. Separation of elevation image into images of (a) lower or flat and (b) sloped roof parts.

First the lower and flat parts of the roof are separated from the sloped parts. In order to test the hypothesis (iii) the gradient field of the elevation image is calculated. Different orientations of the gradient are displayed in Fig. 10a by different brightness values. From the orientation of the gradients possessing a minimum absolute value, a histogram is determined (Fig. 10b). In the histogram we search for peaks in order to determine major orientations and orientation intervals around them.

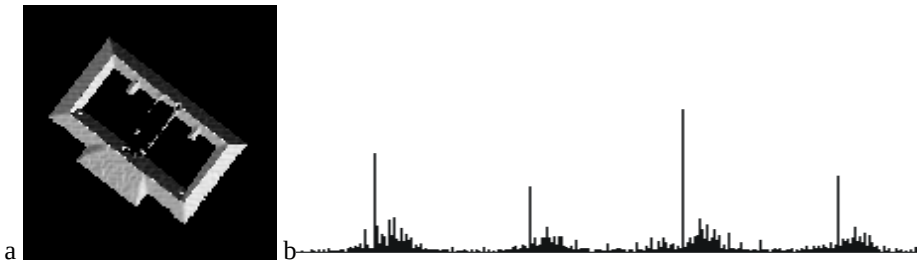

Fig. 10. Orientation of gradient. a) orientation image, b) histogram of orientations

By thresholding the orientation image (Fig. 10a) at the boundaries of the orientation intervals (Fig. 10b), segments of similar orientation are separated. The areas resulting from the segmentation are then morphologically dilated and eroded to fill small unknown enclosed areas, remove small regions, and separate components, which are connected only by a few pixels.

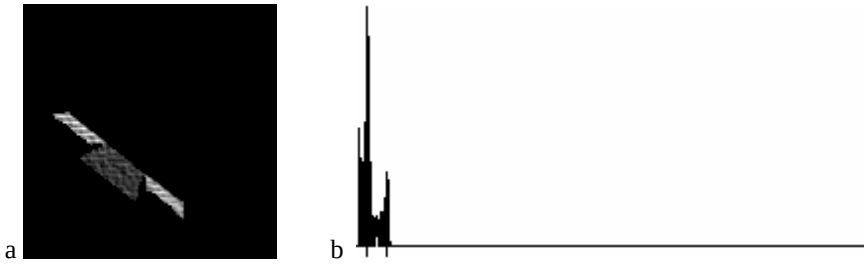

Fig. 11. Separated segment. a) absolute value of gradient, b) histogram.

These segments of homogeneous oriented gradients may still contain areas of different slopes. For an obtained segment Fig. 11a shows the absolute values of

gradients by corresponding brightness values. To separate such connected areas, the histogram of the slope is determined (Fig. 11b). If the distribution shows several significant peaks essentially differing in slope, then the segment is split into the corresponding areas. The result of the segmentation process is shown in Fig. 12.

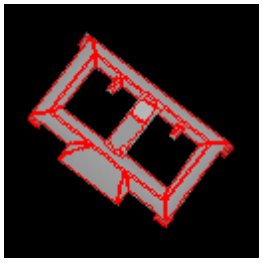

Fig. 12. Segmented elevation image.

Using segments of homogenous orientation and slope, spatial planes are calculated by a least square fit. Recalculating the z-coordinate for the contour points by the plane equation, we ensure a plain 3D contour chain (Fig. 13).

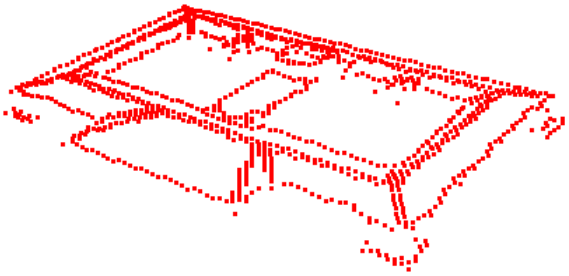

Fig. 13. 3D contour chains

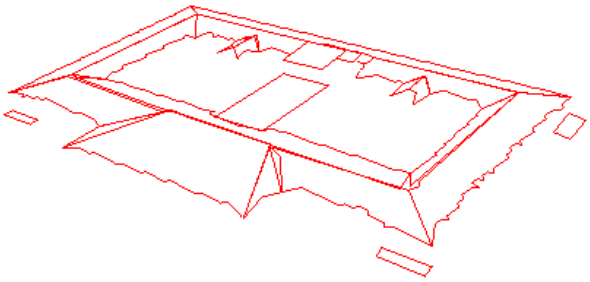

Fig. 14. 3D polygons of roof segments

A polygonal description is obtained by deleting points of the 3D contour chain (Fig. 14). Special attention is required at the neighboring edges of pairs of segments to receive a common line. Since edges of neighboring segments do not intersect in exactly one point, a common vertex has to be calculated. After this step, it may

happen, that points of the bordering polygon do not exactly lie in a plane. In a following tessellation step the surface is split in further planar surfaces. The result of the reconstruction is shown in Fig. 15.

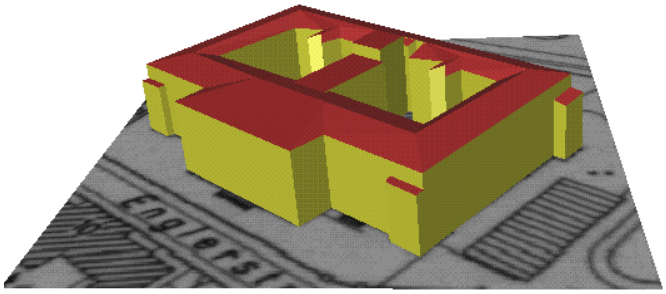

Fig. 15. Reconstructed sloped roof structure

5 Update of City Models

For updating the database of the 3D-city model we propose a procedure in two phases. In a verification phase the buildings which are already stored in the database are compared with the new elevation data by histogram characteristics. They are confirmed, modified or deleted.

In a classification phase new buildings are searched in the elevation data of non-buildings (Fig. 4h). The discrimination of artificial objects from natural objects can be done taking into account the difference in reflectance, elevation texture, local variance of surface gradients, vertical structure (elevation), and shape of the object surfaces (Hug and Wehr, 1997).

One possibility for finding man-made objects is to search for regular structures. For this purpose the elevation data is thresholded appr. 2m above the ground. The resulting binary segments are examined for compactness. In the contour of compact segments we search for basic right-angled structures. A model for composing basic right-angled structures is described in (Stilla et al., 1998).

6 Discussion

The proposed method can be applied to reconstruct complex roof shapes from maps and elevation data. The approach allows the recognition of additional structures (e.g. superstructures) which can not be derived from the building outlines shown in the map. It has been shown, that elevation histograms of laser altimeter data show characteristic features of roofs.

However, the reconstruction of small roof segments is not reliable. Those segments remain unconsidered or are reconstructed as prismatic objects. Additionally, difficulties occur when analyzing histograms of strongly sloped roof segments (high roof) oriented parallel to the grid. They show a set of peaks and look like a comb.

Using the segmentation approach, we have assumed, that roof parts have similar orientations and for the whole roof only a few orientations exists. If the histogram does not show a few major orientations, local relations have to be considered for reconstructing planar surfaces (Besl, 1988). Several segmentation algorithms which are based on region growing are described and compared in (Hoover et al., 1996).

Important for reconstruction is the evaluation of the results. For a quantitative evaluation, ground truths of a set of buildings and task-dependent assessment functions are necessary. Up to now only single objects are qualitatively evaluated. A comparison of the results with a measured CAD-Model is shown in Fig. 16.

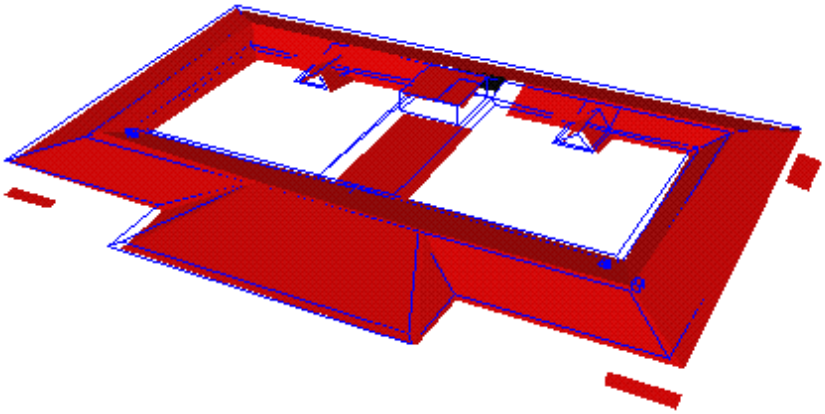

Fig. 16. Comparison of reconstructed segments and truth data (lines)

References

1. Adrian G, Fiedler F (1991) Simulation of unstationary wind and temperatur fields over complex terrain and comparison with observations. Beitr. Phys. Atmosph., 64, 27-48
2. Besl PJ (1988) Surfaces in range image understanding. New York: Springer
3. Danahy J (1997) A set of visualization data needs in urban environmental planning & design for photogrammetric data. In: Gruen et al. (eds) Automatic extraction of man-made objects from aerial and space images (II), 357-366, Basel: Birkhäuser
4. Gruber M, Kofler M, Leberl F (1997) Managing large 3D urban database contents supporting phototexture and levels of detail. In: Gruen et al. (eds) Automatic extraction of man-made objects from aerial and space images (II), 377-386, Basel: Birkhäuser
5. Gruen A (1998) TOBAGO - a semi-automated approach for the generation of 3-D building models. ISPRS Journal of photogrammetry & remote sensing, 53(2): 108-118

6. Guelch E (1997) Application of semi-automatic building acquisition. In: Gruen A et al. (eds.) Automatic extraction of man-made objects from aerial and space images (II), 129-138, Basel: Birkhäuser
7. Haala N, Brenner C (1997) Interpretation of urban surface models using 2D building information. In: Gruen A et al. (eds.) Automatic extraction of man-made objects from aerial and space images (II), 213-222, Basel: Birkhäuser
8. Hug C, Wehr A (1997) Detecting and identifying topographic objects in laser altimeter data. ISPRS, International archives of photogrammetry and remote sensing, Vol. 32, Part 3-4W2, 19-268.
9. Huising EJ, Gomes Pereira LM (1998) Errors and accuracy estimates of laser data acquired by various laser scanning systems for topographic applications. ISPRS Journal of photogrammetry and remote sensing, 53: 245-261
10. Hoover A, Jean-Baptiste, Jiang X, Flynn PJ, Bunke H, Goldof DB, Bowyer K, Eggert DW, Fitzgibbon A, Fisher RB (1996) An experimental comparison of range image segmentation algorithms. IEEE T-PAMI, 16(7):673-689
11. Kakumoto S, Hatayama M, Kameda H, Taniguchi T (1997) Development of disaster management spatial information system. Proc. GIS'97 Conf., 595-598
12. Kürner T, Cichon DJ, Wiesbeck W (1993) Concepts and results for 3D digital terrain-based wave propagation models: An overview. IEEE Journal on selected areas in communications, 11: 1002-1012
13. Lemmens MJPM, Deijkers H, Looman PAM (1997) Building detection by fusing airborne laser-altimeter DEMs and 2D digital maps. ISPRS, International archives of photogrammetry and remote sensing, Vol. 32, Part 3-4W2, 42-49
14. Lohr U (1998) Laserscan DEM for various applications. In: Fritsch D, Englich M, Sester M (eds) GIS - Between Visions and Applications. ISPRS, International archives of photogrammetry and remote sensing, Vol. 32, Part 4, 353-356
15. Stilla U (1995) Map-aided structural analysis of aerial images. ISPRS Journal of Photogrammetry and Remote Sensing, 50(4): 3-10
16. Stilla U, Michaelsen E, Lütjen K (1996) Automatic extraction of buildings from aerial images. In: Leberl F, Kalliany R, Gruber M (eds) Mapping buildings, roads and other man-made structures from images, IAPR-TC7. Wien: Oldenburg, 229-244
17. Stilla U, Michaelsen E (1997) Semantic modeling of man-made objects by production nets. In: Gruen A, Baltsavias EP, Henricsson O (eds) Automatic extraction of man-made objects from aerial and space images (II). Basel: Birkhäuser, 43-52
18. Stilla U, Michaelsen E, Jurkiewicz K (1998) Structural analysis of right-angled building contours. ISPRS, International archives of photogrammetry and remote sensing, Vol. 32, Part 3/1, 379-386
19. Shibasaki R (1998) Proceedings of UM3'98, International Workshop on Urban Multi-Media/3D Mapping., University of Tokyo, Institute of Industrial Science.
20. Weidner U, Förstner W (1995) Towards automatic building extraction from high-resolution digital elevation models. ISPRS Journal of photogrammetry and remote sensing, 50(4): 38-49